Research Article | Vol. 25, No. 4 | 20 Feb 2017 | OPTICS EXPRESS 3311

Optics EXPRESS

Modulation format dependence of digital nonlinearity compensation performance in optical fibre communication systems

Tianhua Xu,[1,*] Nikita A. Shevchenko,[1] Domaniç Lavery,[1] Daniel Semrau,[1] Gabriele Liga,[1] Alex Alvarado,[2] Robert I. Killey,[1] and Polina Bayvel[1]

[1]*Optical Networks Group, Department of Electronic and Electrical Engineering, University College London (UCL), London, WC1E 7JE, UK*
[2]*Signal Processing Systems Group, Department of Electrical Engineering, Eindhoven University of Technology (TU/e), Eindhoven, 5600 MB, The Netherlands*
[*]*tianhua.xu@ucl.ac.uk*

Abstract: The relationship between modulation format and the performance of multi-channel digital back-propagation (MC-DBP) in ideal Nyquist-spaced optical communication systems is investigated. It is found that the nonlinear distortions behave independent of modulation format in the case of full-field DBP, in contrast to the cases of electronic dispersion compensation and partial-bandwidth DBP. It is shown that the minimum number of steps per span required for MC-DBP depends on the chosen modulation format. For any given target information rate, there exists a possible trade-off between modulation format and back-propagated bandwidth, which could be used to reduce the computational complexity requirement of MC-DBP.

OCIS codes: (060.2330) Fiber optics communications; (060.1660) Coherent communications; (060.4370) Nonlinear optics, fibers.

References and links

1. M. Secondini, E. Forestieri, and G. Prati, "Achievable information rate in nonlinear WDM fiber-optic systems with arbitrary modulation formats and dispersion maps," J. Lightwave Technol. **31**(23), 3839–3852 (2013).
2. D. Semrau, T. Xu, N. A. Shevchenko, M. Paskov, A. Alvarado, R. I. Killey, and P. Bayvel, "Achievable information rates estimates in optically amplified transmission systems using nonlinearity compensation and probabilistic shaping," Opt. Lett. **42**(1), 121–124 (2017).
3. P. Bayvel, R. Maher, T. Xu, G. Liga, N. A. Shevchenko, D. Lavery, A. Alvarado, and R. I. Killey, "Maximizing the optical network capacity," Philos Trans A Math Phys Eng Sci **374**(2062), 20140440 (2016).
4. G. P. Agrawal, *Fiber-optic communication systems, 4th ed.* (John Wiley & Sons, Inc., 2010).
5. R.-J. Essiambre and R. W. Tkach, "Capacity trends and limits of optical communication networks," Proc. IEEE **100**(5), 1035–1055 (2012).
6. P. P. Mitra and J. B. Stark, "Nonlinear limits to the information capacity of optical fibre communications," Nature **411**(6841), 1027–1030 (2001).
7. E. M. Ip and J. M. Kahn, "Compensation of dispersion and nonlinear impairments using digital backpropagation," J. Lightwave Technol. **26**(20), 3416–3425 (2008).
8. E. Temprana, E. Myslivets, B. P.-P. Kuo, L. Liu, V. Ataie, N. Alic, and S. Radic, "APPLIED OPTICS. Overcoming Kerr-induced capacity limit in optical fiber transmission," Science **348**(6242), 1445–1448 (2015).
9. F. P. Guiomar, J. D. Reis, A. L. Teixeira, and A. N. Pinto, "Mitigation of intra-channel nonlinearities using a frequency-domain Volterra series equalizer," Opt. Express **20**(2), 1360–1369 (2012).
10. I. D. Phillips, M. Tan, M. F. C. Stephens, M. E. McCarthy, E. Giacoumidis, S. Sygletos, P. Rosa, S. Fabbri, S. T. Le, T. Kanesan, S. K. Turitsyn, N. J. Doran, P. Harper, and A. D. Ellis, "Exceeding the nonlinear-Shannon limit using Raman laser based amplification and optical phase conjugation," in *Proceedings of Optical Fiber Communications Conference*, (Optical Society of America, 2014), paper M3C.1.
11. M. I. Yousefi and F. R. Kschischang, "Information transmission using the nonlinear Fourier transform, Part I-III: Numerical methods," IEEE Trans. Inf. Theory **60**(7), 4329–4345 (2014).
12. X. Liu, A. R. Chraplyvy, P. J. Winzer, R. W. Tkach, and S. Chandrasekhar, "Phase-conjugated twin waves for communication beyond the Kerr nonlinearity limit," Nat. Photonics **7**(7), 560–568 (2013).

#279659 https://doi.org/10.1364/OE.25.003311
Journal © 2017 Received 15 Nov 2016; revised 11 Jan 2017; accepted 12 Jan 2017; published 8 Feb 2017

Optics EXPRESS

13. D. Rafique, "Fiber nonlinearity compensation: commercial applications and complexity analysis," J. Lightwave Technol. **34**(2), 544–553 (2016).
14. S. Randel, P. Winzer, A. Sureka, S. Chandrasekhar, N. K. Fontaine, R. Delbue, R. Ryf, P. Pupalaikis, and X. Liu, "Fiber nonlinearity compensation by digital backpropagation of an entire 1.2 Tb/s superchannel using a full-field spectrally-sliced receiver," in *Proceedings of Optical Fiber Communications Conference*, (Optical Society of America, 2013), paper Mo.3.D.5.
15. A. Napoli, Z. Maalej, V. A. J. M. Sleiffer, M. Kuschnerov, D. Rafique, E. Timmers, B. Spinnler, T. Rahman, L. D. Coelho, and N. Hanik, "Reduced complexity digital back-propagation methods for optical communication systems," J. Lightwave Technol. **32**(7), 1351–1362 (2014).
16. G. Liga, T. Xu, A. Alvarado, R. I. Killey, and P. Bayvel, "On the performance of multichannel digital backpropagation in high-capacity long-haul optical transmission," Opt. Express **22**(24), 30053–30062 (2014).
17. R. Maher, T. Xu, L. Galdino, M. Sato, A. Alvarado, K. Shi, S. J. Savory, B. C. Thomsen, R. I. Killey, and P. Bayvel, "Spectrally shaped DP-16QAM super-channel transmission with multi-channel digital back-propagation," Sci. Rep. **5**, 8214 (2015).
18. X. Liu, S. Chandrasekhar, and P. J. Winzer, "Digital signal processing techniques enabling multi-Tb/s superchannel transmission: an overview of recent advances in DSP-enabled superchannels," IEEE Signal Process. Mag. **31**(2), 16–24 (2014).
19. T. Xu, G. Liga, D. Lavery, B. C. Thomsen, S. J. Savory, R. I. Killey, and P. Bayvel, "Equalization enhanced phase noise in Nyquist-spaced superchannel transmission systems using multi-channel digital back-propagation," Sci. Rep. **5**, 13990 (2015).
20. T. Fehenberger, A. Alvarado, P. Bayvel, and N. Hanik, "On achievable rates for long-haul fiber-optic communications," Opt. Express **23**(7), 9183–9191 (2015).
21. Z. Liu, S. Farwell, M. Wale, D. J. Richardson, and R. Slavík, "InP-based optical comb-locked tunable transmitter," in *Proceedings of Optical Fiber Communications Conference*, (Optical Society of America, 2016), paper Tu2K.2.
22. G. Bosco, A. Carena, V. Curri, R. Gaudino, P. Poggiolini, and S. Benedetto, "Suppression of spurious tones induced by the split-step method in fiber systems simulation," IEEE Photonics Technol. Lett. **12**(5), 489–491 (2000).
23. R. Kudo, T. Kobayashi, K. Ishihara, Y. Takatori, A. Sano, and Y. Miyamoto, "Coherent optical single carrier transmission using overlap frequency domain equalization for long-haul optical systems," J. Lightwave Technol. **27**(16), 3721–3728 (2009).
24. T. Xu, G. Jacobsen, S. Popov, J. Li, E. Vanin, K. Wang, A. T. Friberg, and Y. Zhang, "Chromatic dispersion compensation in coherent transmission system using digital filters," Opt. Express **18**(15), 16243–16257 (2010).
25. G. P. Agrawal, *Nonlinear fibre optics, 5th ed.* (Academic Press, 2013).
26. P. Poggiolini, "The GN model of non-linear propagation in uncompensated coherent optical systems," J. Lightwave Technol. **30**(24), 3857–3879 (2012).
27. P. Johannisson and M. Karlsson, "Perturbation analysis of nonlinear propagation in a strongly dispersive optical communication system," J. Lightwave Technol. **31**(8), 1273–1282 (2013).
28. P. Poggiolini, G. Bosco, A. Carena, V. Curri, Y. Jiang, and F. Forghieri, "The GN-Model of fiber non-linear propagation and its applications," J. Lightwave Technol. **32**(4), 694–721 (2014).
29. D. Rafique and A. D. Ellis, "Impact of signal-ASE four-wave mixing on the effectiveness of digital back-propagation in 112 Gb/s PM-QPSK systems," Opt. Express **19**(4), 3449–3454 (2011).
30. L. Beygi, N. V. Irukulapati, E. Agrell, P. Johannisson, M. Karlsson, H. Wymeersch, P. Serena, and A. Bononi, "On nonlinearly-induced noise in single-channel optical links with digital backpropagation," Opt. Express **21**(22), 26376–26386 (2013).
31. N. A. Shevchenko, T. Xu, D. Semrau, G. Saavedra, G. Liga, M. Paskov, L. Galdino, A. Alvarado, R. I. Killey, and P. Bayvel, "Achievable information rates estimation for 100-nm Raman-amplified optical transmission system," in *Proceedings of European Conference on Optical Communication (ECOC)*, (Institute of Electrical and Electronics Engineers, 2016), pp. 878–880.
32. A. Mecozzi and R.-J. Essiambre, "Nonlinear Shannon limit in pseudolinear coherent systems," J. Lightwave Technol. **30**(12), 2011–2024 (2012).
33. R. Dar, M. Feder, A. Mecozzi, and M. Shtaif, "Properties of nonlinear noise in long, dispersion-uncompensated fiber links," Opt. Express **21**(22), 25685–25699 (2013).
34. A. Bononi and P. Serena, "On the accuracy of the Gaussian nonlinear model for dispersion-unmanaged coherent links," in *Proceedings of European Conference on Optical Communication (ECOC)*, (Institute of Electrical and Electronics Engineers, 2013), paper Th.1.D.3.
35. P. Serena, A. Bononi, and N. Rossi, "The impact of the modulation dependent nonlinear interference missed by the Gaussian noise model," in *Proceedings of European Conference on Optical Communication (ECOC)*, (Institute of Electrical and Electronics Engineers, 2014), paper Mo.4.3.1.
36. R. Dar, M. Feder, A. Mecozzi, and M. Shtaif, "Accumulation of nonlinear interference noise in fiber-optic systems," Opt. Express **22**(12), 14199–14211 (2014).
37. A. Carena, G. Bosco, V. Curri, Y. Jiang, P. Poggiolini, and F. Forghieri, "EGN model of non-linear fiber propagation," Opt. Express **22**(13), 16335–16362 (2014).

Optics EXPRESS

38. P. Poggiolini, G. Bosco, A. Carena, V. Curri, Y. Jiang, and F. Forghieri, "A simple and effective closed-form GN model correction formula accounting for signal non-Gaussian distribution," J. Lightwave Technol. **33**(2), 459–473 (2015).
39. T. Tanimura, M. Nölle, J. K. Fischer, and C. Schubert, "Analytical results on back propagation nonlinear compensator with coherent detection," Opt. Express **20**(27), 28779–28785 (2012).
40. J. C. Cartledge, F. P. Guiomar, F. R. Kschischang, G. Liga, and M. P. Yankov, "Digital signal processing for fiber nonlinearities," Opt. Express (to appear).
41. P. Poggiolini, Y. Jiang, A. Carena, and F. Forghieri, "Analytical modeling of the impact of fiber non-linear propagation on coherent systems and networks," Chapter 7 in Enabling Technologies for High Spectral-efficiency Coherent Optical Communication Networks, 247–309 (2016).
42. R. Dar, M. Feder, A. Mecozzi, and M. Shtaif, "Inter-channel nonlinear interference noise in WDM systems: modeling and mitigation," J. Lightwave Technol. **33**(5), 1044–1053 (2015).
43. L. Szczecinski and A. Alvarado, *Bit-Interleaved Coded Modulation: Fundamentals, Analysis and Design* (John Wiley & Sons, Inc., 2015).
44. D. Arnold, H.-A. Loeliger, P. Vontobel, A. Kavcic, and W. Zeng, "Simulation-based computation of information rates for channels with memory," IEEE Trans. Inf. Theory **52**(8), 3498–3508 (2006).
45. M. Secondini, S. Rommel, G. Meloni, F. Fresi, E. Forestieri, and L. Potì, "Single-step digital backpropagation for nonlinearity mitigation," Photonic Netw. Commun. **31**(3), 493–502 (2016).
46. M. Secondini, S. Rommel, F. Fresi, E. Forestieri, G. Meloni, and L. Potì, "Coherent 100G nonlinear compensation with single-step digital backpropagation," in *Proceedings of International Conference on Optical Network Design and Modeling (ONDM)*, (Institute of Electrical and Electronics Engineers, 2015), pp. 63–67.

1. Introduction

Currently, over 95% of digital data traffic is carried over optical fibre networks, which form a substantial part of the national and international communication infrastructure. The achievable information rates (AIRs), a natural figure of merit in coded communication systems for demonstrating the net data rates based on soft-decision decoding [1,2], of optical fibre networks have increased greatly over the past four decades with the introduction and development of wavelength division multiplexing (WDM), advanced modulation formats, digital signal processing (DSP), improved optical fibres and amplifier technologies, which together have facilitated the communication revolution and the growth of the Internet [3,4]. However, the AIRs of optical communication systems are currently limited by the nonlinear distortions inherent to transmission using optical fibres. These signal degradations are more significant in systems using larger transmission bandwidths, closer channel spacing and higher order modulation formats. Optical fibre nonlinearities have been suggested as the major bottleneck to optical fibre transmission performance [5,6].

Much research work is focused on compensating fibre nonlinearities both electronically and optically to enhance the AIRs of optical communication systems. A number of nonlinear compensation (NLC) techniques have been investigated, such as digital back-propagation (DBP), nonlinear pre-distortion, Volterra equalisation, optical phase conjugation, nonlinear Fourier transform, twin-wave phase conjugation, etc [7–13]. Among these, multi-channel DBP (MC-DBP) has been validated as a promising approach for compensating both intra-channel and inter-channel fibre nonlinearities in WDM optical communication systems. The performance and optimisation of MC-DBP have been investigated separately in both dual-polarisation 16-*ary* quadrature amplitude modulation (DP-16QAM) and DP-64QAM transmission systems [14–19], where the minimum required number of steps per span (MRNSPS), an important complexity index in MC-DBP, to achieve the greatest Q^2 factors/lowest bit-error-rates (BERs) at different back-propagated bandwidths was studied. In addition, the performance of single-channel and full-field DBP with regard to the AIRs has been studied for 16-QAM and 64-QAM systems [20]. However, to the best of our knowledge, no optimisations and analytical predictions for partial-bandwidth DBP were comprehensively investigated with respect to AIRs over different signal modulation formats.

In this paper, the performance and the optimisation of MC-DBP is studied with respect to both signal-to-noise ratios (SNRs) and AIRs of the compensated optical fibre communication systems, where different modulation formats, including dual-polarisation quadrature phase shift keying (DP-QPSK), DP-16QAM, DP-64QAM, DP-256QAM, are applied. Numerical

Optics EXPRESS

simulations and analytical modelling have been carried out in a reference system of a 9-channel 32-Gbaud Nyquist-spaced WDM optical communication system, with a transmission link of standard single-mode fibre (SSMF). Additionally, the MRNSPS, which is an important index for assessing the complexity of MC-DBP algorithm [7,13,14], has been studied with respect to the AIRs of the compensated communication systems. Finally, an analytical model for predicting the performance of EDC, partial-bandwidth DBP, and full-field DBP in the optical transmission system has been implemented by considering the contribution of modulation format dependent nonlinear distortions.

It is found that the nonlinear distortions in the systems with applying full-field DBP (due to signal-noise interactions) become independent of modulation format, while the nonlinear distortions in both the electronic dispersion compensation (EDC) and partial-bandwidth DBP (mainly from signal-signal interactions) display a considerable dependence on modulation format. In the optimisation with respect to AIRs, the MRNSPS at different back-propagated bandwidths demonstrates a strong dependence on the modulation format, in comparison with the optimisation of MC-DBP based on SNRs. Also, for any given target information rate, there exists a possible trade-off between modulation format and back-propagated bandwidth which could be used to reduce the computational complexity requirement of MC-DBP.

This paper is arranged as follows. The transmission system under investigation and numerical simulation setup are described in Section 2. The analytical transmission model and mutual information theory is outlined in Section 3. Section 4 details the simulation and analytical results, and further analyses the MRNSPS and the AIRs for different modulation formats in several scenarios of interest. Finally, conclusions are drawn in Section 5.

2. Transmission system

Figure 1 illustrates the simulation setup of the 9-channel 32-Gbaud Nyquist-spaced superchannel optical transmission system using the following modulation formats: DP-QPSK, DP-16QAM, DP-64QAM and DP-256QAM. In the transmitter, a 9-line 32-GHz spaced laser comb is employed as the phase-locked optical carrier, and the comb lines are optically de-multiplexed before the I-Q modulators [8,21]. The transmitted symbol sequence in each optical channel is independent and random, and the symbol sequences in each polarisation are de-correlated with a delay of half the sequence length. A root-raised cosine (RRC) filter with a roll-off of 0.1% is used for the Nyquist pulse shaping (NPS). The SSMF is simulated based on the split-step Fourier solution of the Manakov equation with a logarithmic step-size distribution, of which the mathematical expression can be found in Eq. (6) in Ref [22]. The erbium-doped optical fibre amplifier (EDFA) is employed in the loop to compensate for the loss in the optical fibre. At the receiver, the signal is mixed with an ideal free-running local oscillator (LO) laser to realise an ideal coherent detection of all in-phase and quadrature signal components in each polarisation.

In the DSP modules, the EDC is implemented using a frequency domain equaliser [23,24], and the MC-DBP is realised using the reverse split-step Fourier solution of Manakov equation with the nonlinearity compensation implemented in the middle of each segment [7,16,25]. The ideal RRC filter is applied to select the desired back-propagated bandwidth for the MC-DBP, and also to remove the unwanted out-of-band amplified spontaneous emission (ASE) noise. The back-propagated bandwidths considered are from 32-GHz for the 1-channel DBP, increasing to 288-GHz for 9-channel (hereafter, full-field) DBP. The matched filter is employed to select the central channel and to remove cross talk from neighbouring channels. Finally, the SNR is estimated over 2^{18} symbols to assess the performance of the central channel, and the mutual information (MI) is further computed from the SNR, as discussed in Section 3.2. All numerical simulations are implemented with a digital resolution of 18 sample/symbol. The phase noise from the transmitter and LO lasers, the frequency offset of the transmitter and LO lasers, as well as the differential group delay (DGD) between the two

Optics EXPRESS

polarisations in the fibre are all neglected. Detailed parameters of the optical transmission system are shown in Table 1.

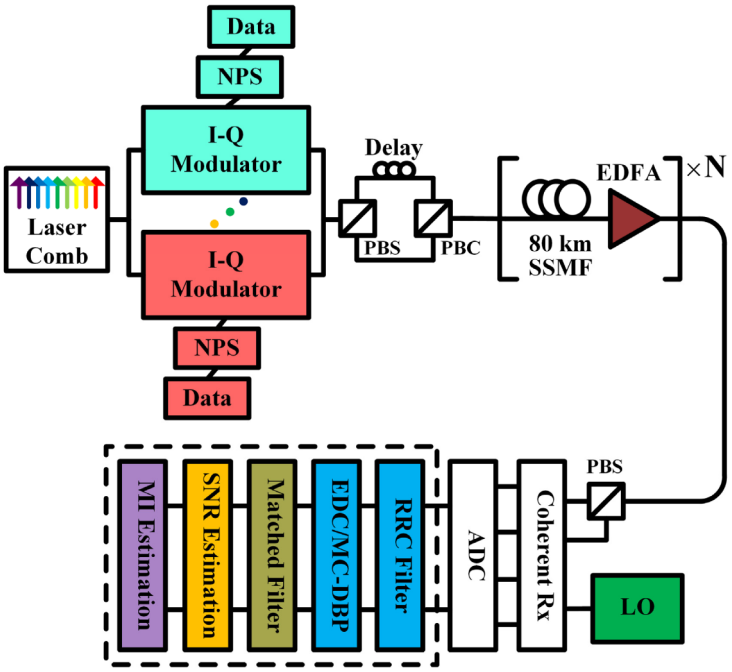

Fig. 1. Schematic of the 9-channel Nyquist-spaced optical fibre communication system using EDC and MC-DBP. (NPS: Nyquist pulse shaping, PBS: polarisation beam splitter, PBC: polarisation beam combiner, LO: local oscillator, ADC: analogue-to-digital convertor, MI: mutual information)

Table 1. Transmission System Parameters

Parameter	Value
Symbol rate	32 Gbaud
Channel spacing	32 GHz
Central wavelength (both transmitter and LO)	1550 nm
Number of channels	9
Roll-off	0.1%
Attenuation coefficient (α)	0.2 dB/km
Chromatic dispersion coefficient (D)	17 ps/nm/km
Nonlinear coefficient (γ)	1.2 /W/km
Span length	80 km
Number of spans	25
SSMF steps per span (logarithmic step-size)	800
EDFA noise figure	4.5 dB
Simulation bandwidth	576 GHz

3. Analytical model and AIR estimation

3.1 Nonlinear distortions in the optical communication system

Considering the contributions from ASE noise and fibre nonlinearities (optical Kerr effect), the performance of a dispersion-unmanaged optical communication system can be described using a so-called effective SNR [26,27], which after fibre propagation can be described as

$$\mathrm{SNR} = \frac{P}{\sigma_{\mathrm{eff}}^2} \approx \frac{P}{\sigma_{\mathrm{ASE}}^2 + \sigma_{\mathrm{S-S}}^2 + \sigma_{\mathrm{S-N}}^2}, \tag{1}$$

Optics EXPRESS

where P is the average optical power per channel, σ^2_{ASE} represents the total power of ASE noise within the examined channel due to the optical amplification process, $\sigma^2_{\mathrm{S-S}}$ represents the distortions due to signal-signal nonlinear interactions, and $\sigma^2_{\mathrm{S-N}}$ represents the distortions from signal-ASE noise interactions.

For dual-polarisation multi-span EDFA amplified Nyquist-spaced WDM transmission systems, the overall ASE noise exhibits as an additive white Gaussian noise coming from EDFAs at the end of each transmission span and can be expressed as [4]

$$\sigma^2_{\mathrm{ASE}} = N_{\mathrm{s}}\left(G-1\right)F_n\, h\nu_0\, R_S, \tag{2}$$

where N_{s} is the total number of spans in the link, G is the EDFA gain, F_n is the EDFA noise figure, $h\nu_0$ is the average photon energy at the optical carrier frequency ν_0, and R_S denotes the symbol rate of the transmitted signal. The contribution of the nonlinear distortions due to nonlinear signal-signal interaction can be described as follows [26–28]

$$\sigma^2_{\mathrm{S-S}} = N_{\mathrm{s}}^{\varepsilon+1}\,\eta P^3, \tag{3}$$

where η is the nonlinear distortion coefficient, ε is the coherence factor, which is responsible for the increasing signal-signal interaction with transmission distance. This factor lies between 0 and 1 depending on the decorrelation of the nonlinear distortions between each fibre span [26]. In contrast to the $\sigma^2_{\mathrm{S-S}}$ term, the corresponding noise contribution due to signal-ASE interaction grows quadratically with launched power [29,30], and can be modelled as:

$$\sigma^2_{\mathrm{S-N}} \approx 3\varsigma\eta\,\sigma^2_{\mathrm{ASE}}\,P^2, \tag{4}$$

with the distance dependent pre-factor of ς, which accounts for the accumulation of signal-ASE distortions with the transmission distance, and can be effectively truncated as [31]:

$$\varsigma = \sum_{n=1}^{N_{\mathrm{s}}} n^{\varepsilon+1} \approx \frac{N_{\mathrm{s}}^{\varepsilon+1}}{2} + \frac{N_{\mathrm{s}}^{\varepsilon+2}}{\varepsilon+2}. \tag{5}$$

In the framework of the first-order perturbation theory, the coefficient η can be defined depending on the model assumptions. In the conventional approaches, the impact of optical fibre nonlinearities on signal propagation is typically treated as additive circularly symmetric Gaussian noise [6,26,27]. In particular, the effective variance of nonlinear distortions is clearly supposed to be entirely independent of the signal modulation format. However, it has been theoretically shown that the nonlinear distortions depend on the channel input symbols, and the Gaussian assumption of optical nonlinear distortions cannot, therefore, be sufficiently accurate [1,32–37]. Furthermore, significant discrepancies have been recently observed, especially for low-order signal modulation formats [33–36]. Assuming that all WDM channels are equally-spaced, the modulation format dependent nonlinear distortion coefficient η over a single fibre span can be expressed in closed-form using the following approximation [38]

$$\eta\left(N_{\mathrm{ch}}\right) \approx \eta_0\left(N_{\mathrm{ch}}\right) - \frac{80}{81}\frac{\kappa\gamma^2 L_{\mathrm{eff}}^2}{\pi\left|\beta_2\right| L_{\mathrm{s}} R_S^2}\left[\psi\left(\frac{N_{\mathrm{ch}}+1}{2}\right) + C + 1\right], \tag{6}$$

where β_2 is the group velocity dispersion coefficient, γ is the fibre nonlinear coefficient, L_{eff} is the effective fibre span length, L_{s} is the fibre span length, N_{ch} is the total number of WDM channels, $\psi(x)$ is the digamma function, $C\approx 0.577$ is the Euler-Mascheroni constant. The constant κ is related to the fourth standardised moment (kurtosis) of the input signal constellation. For Gaussian, QPSK, 16-QAM, 64-QAM, and 256-QAM, its values are {0, 1,

Optics EXPRESS

17/25, 13/21, 121/200}, respectively [36,38]. Finally, the coefficient η_0 quantifies the influence of optical fibre nonlinearity per fibre span under the Gaussian assumption, and can be analytically approximated as [26–28]

$$\eta_0\left(N_{\mathrm{ch}}\right) \approx \left(\frac{2}{3}\right)^3 \frac{\alpha\gamma^2 L_{\mathrm{eff}}^2}{\pi\left|\beta_2\right| R_S^2} \operatorname{ar\,sin\,h}\left(\frac{\pi^2}{2}\left|\beta_2\right| L_{\mathrm{eff}} \cdot N_{\mathrm{ch}}^2 R_S^2\right), \tag{7}$$

where α is the fibre attenuation parameter.

It should be noted that the signal-signal interaction term in Eq. (1) can be completely suppressed via full-field nonlinearity compensation. However, similar to [39], when the nonlinearity compensation is partially applied by means of operating the MC-DBP over a certain bandwidth, the residual signal-signal interaction term in Eq. (1) can be effectively modelled as follows

$$\sigma_{\mathrm{S-S}}^2 = N_{\mathrm{s}}^{\varepsilon+1}\left[\eta\left(N_{\mathrm{ch}}\right) - \eta\left(N_{\mathrm{ch}}^{(\mathrm{DBP})}\right)\right] P^3, \tag{8}$$

where $N_{\mathrm{ch}}^{(\mathrm{DBP})}$ denotes the number of back-propagated channels.

Parameters used in the analytical model are specified in Table 2. The effectiveness of the modulation-dependent analytical model for predicting the performance of EDC and MC-DBP has been verified in previous work [36,37,40–42], where detailed comparisons between the analytical and simulation results in terms of SNR have been investigated under various transmission schemes.

Table 2. Parameters in Analytical Model

Parameter	Value
Symbol rate	32 Gbaud
Channel spacing	32 GHz
Central wavelength	1550 nm
Number of channels	9
Roll-off	0%
Attenuation coefficient (α)	0.2 dB/km
CD coefficient (D)	17 ps/nm/km
Nonlinear coefficient (γ)	1.2 /W/km
Span length	80 km
EDFA noise figure	4.5 dB
Planck constant (h)	6.626×10^{-34} J·s
Euler-Mascheroni constant (C)	0.577

3.2 Mutual information and achievable information rate estimation

The discrete-time memoryless additive white Gaussian noise (AWGN) channel with complex-valued input random symbols X and output random symbols Y in each state of polarisation is given by the well-known input-output relationship: $Y = X + Z$, where Z denotes a zero-mean, circularly symmetric, complex-valued, Gaussian random variable (independent of X) with power $\sigma_z^2 = \mathrm{Var}\left[\left|Z\right|\right] = \mathrm{E}\left[\left|Y - X\right|^2\right]$, where $\mathrm{E}[\cdot]$ stands for the mathematical expectation operator. Then, the SNR for the AWGN channel is defined as $\mathrm{SNR} = \sigma_x^2 / \sigma_z^2$, where $\sigma_x^2 = \mathrm{E}\left[\left|X\right|^2\right]$ represents the average transmit power. The dual-polarisation symbol-wise soft-decision mutual information (MI) for a discrete QAM signal input distribution can be numerically computed by its definition as

$$\mathrm{MI} = \frac{2}{M}\sum_{x\in\mathbf{X}}\int_{\mathbf{C}} P_{Y|X}\left(y\,|\,x\right)\log_2\frac{P_{Y|X}\left(y\,|\,x\right)}{\frac{1}{M}\sum_{x'\in\mathbf{X}} P_{Y|X}\left(y\,|\,x'\right)}dy, \tag{9}$$

where the pre-factor of 2 accounts the use of two polarisation states, $\mathbf{X} = [X_1, ..., X_M]$ denotes the set of possible transmitted random symbols, $\mathbf{C}$ denotes the set of complex numbers, $M = |\mathbf{X}| = 2^m$ is the cardinality of the M-QAM constellation with the number of bits per symbol m. Owing to the AWGN channel assumptions, the conditional probability density function of the channel output Y given the channel input X (the channel law) is given by [1,20,43]:

$$P_{Y|X}(y \mid x) = \frac{1}{\pi\sigma_z^2} \exp\left(-\frac{|y-x|^2}{\sigma_z^2}\right). \tag{10}$$

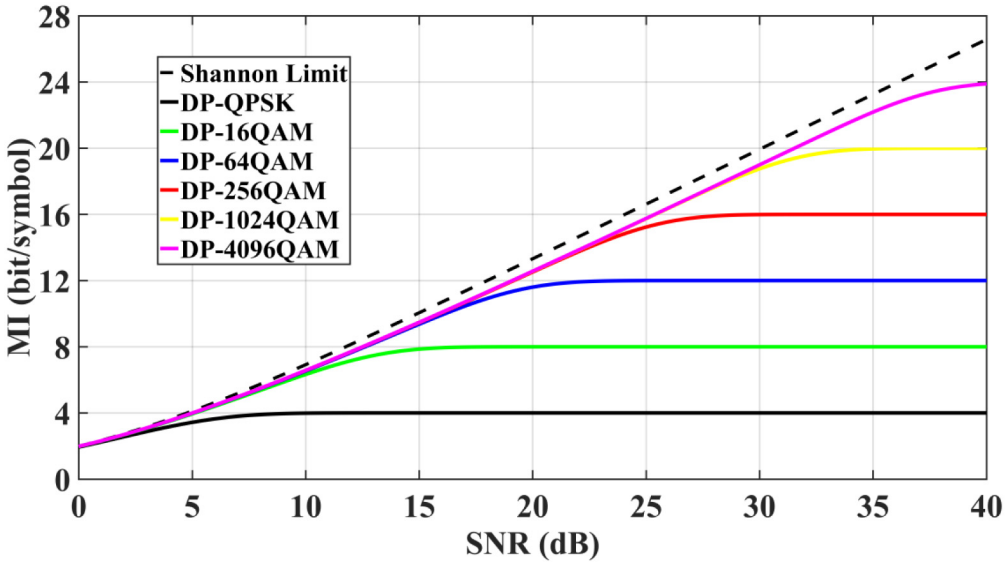

Fig. 2. Theoretical symbol-wise soft-decision MI versus SNR per symbol for dual-polarisation systems using different modulation formats under the assumption of a Gaussian channel law.

The relationship between the symbol-wise soft-decision MI and the SNR for the AWGN channel model is illustrated in Fig. 2, where the MI is numerically computed using Gauss-Hermite quadrature [43]. For a dual-polarisation Nyquist-spaced communication system, the AIR (in bit/s) can be straightforwardly evaluated from the MI as follows:

$$\text{AIR} = N_{\text{ch}} R_S \, \text{MI}. \tag{11}$$

Since the "true" channel law of optical fibre channel is unknown, we follow the concept of mismatched decoding as described in [44]. Thus, we obtain a lower bound on the MI in Eq. (9), assuming that the auxiliary channel is given by Eq. (10), leading to the following approximations for the effective variance in Eq. (1) $\sigma_{\text{eff}}^2 \approx \sigma_z^2$ and the average optical power $P \approx \sigma_x^2$.

4. Results and discussions

In this section, the performance and optimisation of MC-DBP are investigated in terms of both SNR and AIR. The transmission link is 2000 km (25 × 80 km) SSMF, unless otherwise noted. The nonlinear coefficient in the MC-DBP algorithm is always set to 1.2 /W/km, which is the same as in the optical fibre. The simulation results of SNR versus optical signal power per channel at different back-propagated bandwidths is shown in Fig. 3, where different modulation are used. All the MC-DBP algorithms are operated with 800 step/span to ensure

Optics EXPRESS

optimal performance. It is found that the DP-16QAM, DP-64QAM, and DP-256QAM transmission systems behave almost the same, while the DP-QPSK system outperforms the other three modulation formats in the cases of EDC and up to 7-channel DBP. This shows the nonlinear distortions in the EDC and partial-bandwidth DBP case (mainly from signal-signal interactions) depend on modulation format, and the DP-QPSK system has less nonlinear distortions than other modulation formats due to less "Gaussianity" in the QPSK constellation. This is consistent with earlier work [35,36]. However, in the case of full-field (9-channel) DBP, the transmission systems using all modulation formats behave the equivalently, and this demonstrates that the nonlinear distortions (now mainly from signal-noise interactions) become independent of modulation formats in the case of full-field DBP, where the signal-signal nonlinear interactions have been fully compensated.

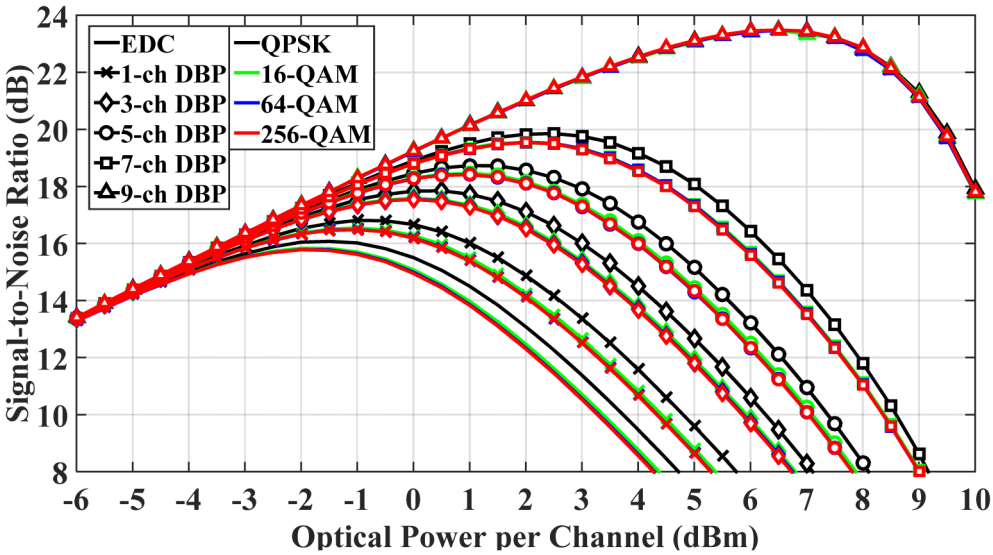

Fig. 3. Simulation results of SNR versus optical launch power at different back-propagated bandwidths for different modulation formats.

Figure 4 shows the simulation results of SNR versus number of steps per span in the MC-DBP algorithm for different back-propagated bandwidths, where different modulation formats are applied. Here the MRNSPS is defined as the minimum number of steps per fibre span to achieve the best system performance (Q^2 factor, SNR or AIR) in MC-DBP for different numbers of back-propagated channels, which is a significant indicator for evaluating the complexity of the MC-DBP algorithm [7,13,14]. It can be seen that, for the same back-propagated bandwidth, the MRNSPS is the same for all modulation formats when the MC-DBP algorithm is optimised in terms of SNR performance, which is 5 steps for 1-channel DBP, 25 for 3-channel DBP, 75 for 5-channel DBP, 150 for 7-channel DBP, and 500 for 9-channel (full-field) DBP. Again, when the MC-DBP is optimised in terms of SNR, the DP-QPSK system outperforms the DP-16QAM, DP-64QAM and DP-256QAM transmission systems in the cases of (linear) EDC and up to 7-channel DBP, and the systems behave the same for all modulation formats in the case of full-field (9-channel) DBP.

Optics EXPRESS

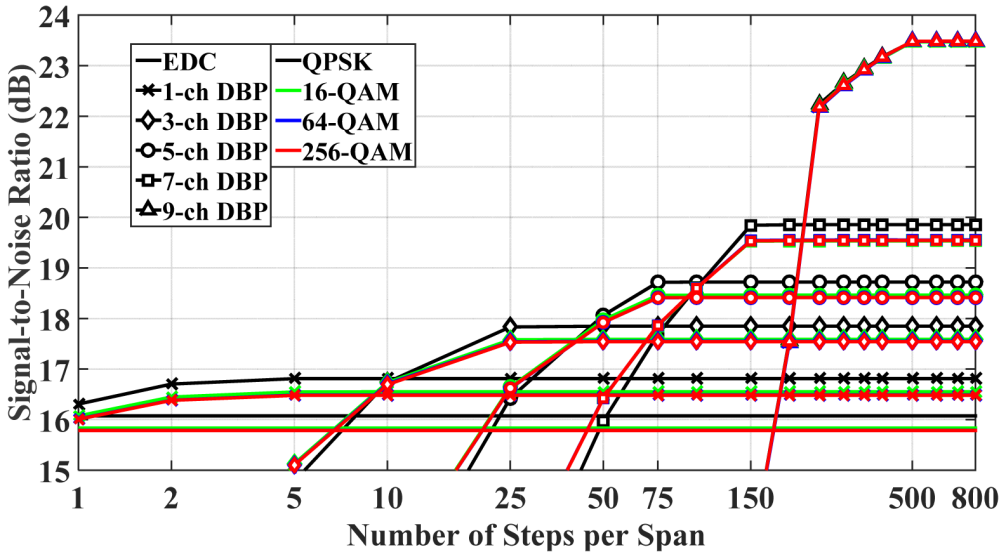

Fig. 4. Simulation results of SNR versus number of steps per span in MC-DBP at different back-propagated bandwidths for different modulation formats.

The above discussions are based on the evaluation and optimisation of the MC-DBP algorithm in terms of SNR performance. However, in the coded transmission systems, the AIR is a more useful indicator and can demonstrate the net data rates that can be achieved by a transceiver based on soft-decision decoding. In the following work the MC-DBP algorithm will be investigated and optimised in terms of AIR.

In Fig. 5, the MRNSPS at different back-propagated bandwidths is studied with respect to the AIRs of the 9-channel 32-Gbaud Nyquist-spaced optical communication system, where different modulation formats are applied. It can be seen that for different back-propagated bandwidths, the MRNSPS in the MC-DBP algorithm depends on the order of the modulation formats, to achieve the best possible AIR. This demonstrates, for the first time to our knowledge, that the MRNSPS depends on the modulation format if MC-DBP is optimised with respect to AIR. The MRNSPS at different back-propagated bandwidths for different modulation formats is shown in Table 3. Compared to the optimisation of MC-DBP with respect to SNR, the DP-256QAM system has the same MRNSPS to achieve the best AIR for different back-propagated bandwidths. However, the MRNSPS in the MC-DBP algorithm for DP-QPSK, DP-16QAM, and DP-64QAM systems is significantly reduced with the decrease in modulation format order.

The MRNSPS in the MC-DBP optimisation with respect to SNR is shown at the bottom of Table 3. It is found that for the DP-QPSK transmission system, the MRNSPS is reduced to (or less than) 1/5 of the MRNSPS in the MC-DBP optimisation in terms of SNR, which means the conventional optimisation actually overestimates the system requirements. This has an implication for practical optimisation of the MC-DBP algorithm that the complexity of MC-DBP may be reduced considerably if it is re-optimised with respect to AIR, depending on the modulation format applied in the communication system.

Optics EXPRESS

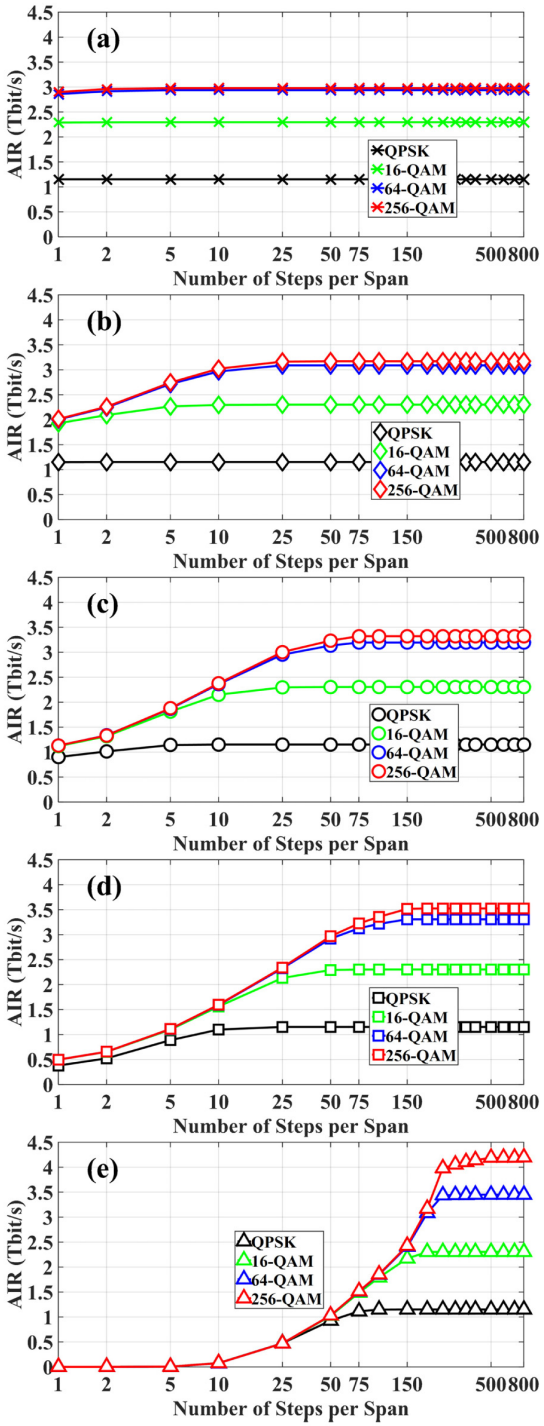

Fig. 5. Simulation results of AIR versus number of steps per span in MC-DBP for different modulation formats. (a) 1-channel DBP (32 GHz), (b) 3-channel DBP (96 GHz), (c) 5-channel DBP (160 GHz), (d) 7-channel DBP (224 GHz), (e) 9-channel DBP (288 GHz).

Optics EXPRESS

Table 3. Minimum required number of steps per span

MRNSPS in terms of AIRs					
Modulation formats	**1-ch DBP**	**3-ch DBP**	**5-ch DBP**	**7-ch DBP**	**9-ch DBP**
DP-QPSK	1	2	5	25	100
DP-16QAM	1	10	25	75	200
DP-64QAM	5	25	75	150	250
DP-256QAM	5	25	75	150	500
MRNSPS in terms of SNRs					
DP-QPSK	5	25	75	150	500
DP-16QAM	5	25	75	150	500
DP-64QAM	5	25	75	150	500
DP-256QAM	5	25	75	150	500

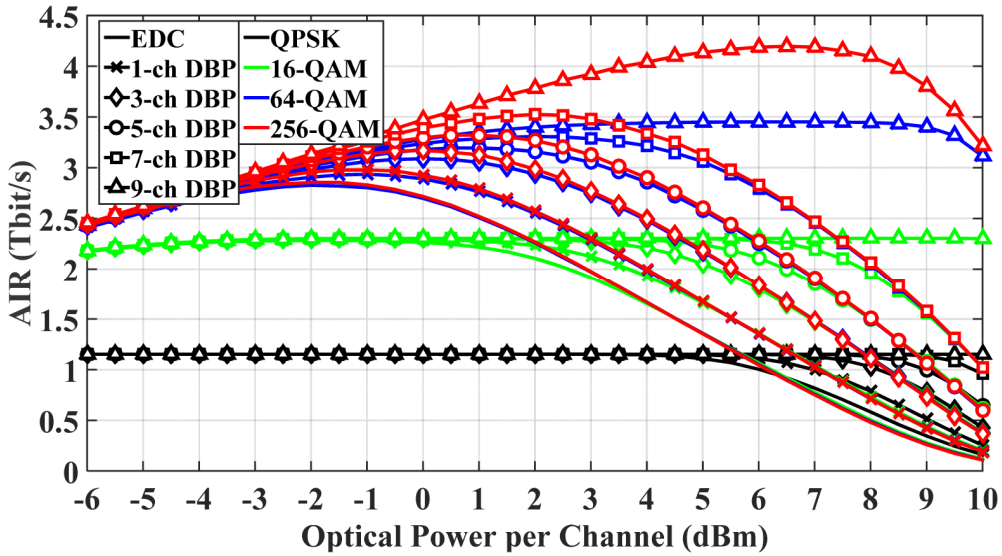

Fig. 6. Simulation results of AIR versus optical launch power at different back-propagated bandwidths for different modulation formats. The transmission distance is 2000 km.

Corresponding to Fig. 2, Fig. 6 shows the simulation results of AIRs versus optical signal power in the 9-channel 32-Gbaud Nyquist-spaced optical fibre communication system using different modulation formats at different back-propagated bandwidths, where all the MC-DBP algorithms have been operated with 800 step/span to ensure optimal performance. Firstly, it can be found that the highest gain in terms of AIRs for the full-field (9-channel) DBP comes from the highest order of modulation formats (DP-256QAM), which is 1.34 Tbit/s from 2.86 Tbit/s at –2 dBm in EDC case to 4.20 Tbit/s at 6.5 dBm in the 9-channel DBP case. It is also found in Fig. 6 that the AIR of the DP-256QAM system using 7-channel DBP exceeds the DP-64QAM system using full-field (9-channel) DBP when the optical power is less than 3.5 dBm, and also exceeds the AIR of the DP-16QAM and DP-QPSK systems using full-field DBP. This implies that, to achieve a given target AIR, there could be a compromise in the selection between the modulation format and the back-propagated bandwidth, depending on the permissible complexity of the system implementation. This effect will depend on the transmission distance and an analytical prediction based on the modulation format dependent noise model is implemented to assess the system performance at different transmission distances.

Optics EXPRESS

As discussed in Section 3, the analytical model for predicting the AIRs of the 9-channel 32-Gbaud Nyquist-spaced optical transmission system using EDC, partial-bandwidth DBP and full-field DBP has been implemented based on the modulation format dependent noise model, where different modulation formats including DP-QPSK, DP-16QAM, DP-64QAM and DP-256QAM are applied. The prediction of AIR at the optimum launch power for different back-propagated bandwidths according to this analytical model and the simulation results are both shown in Fig. 7. The '0' value of the number of back-propagated channels refers to the EDC-only case, and the dots inside the hollow markers of all EDC cases are the analytical predictions. It is found in Fig. 7 that a good agreement has been achieved between the analytical model and the numerical simulations for all modulation formats, in the cases of both EDC and MC-DBP. Figure 7 also indicates that DBP provides no gain in terms of AIR at the optimum power in the DP-QPSK and DP-16QAM optical communication systems at the transmission distance of 2000 km. This is because the MIs at the optimum SNR in the case of EDC have already reached their maximum values in Fig. 2, for the 2000 km DP-QPSK and DP-16QAM transmission systems.

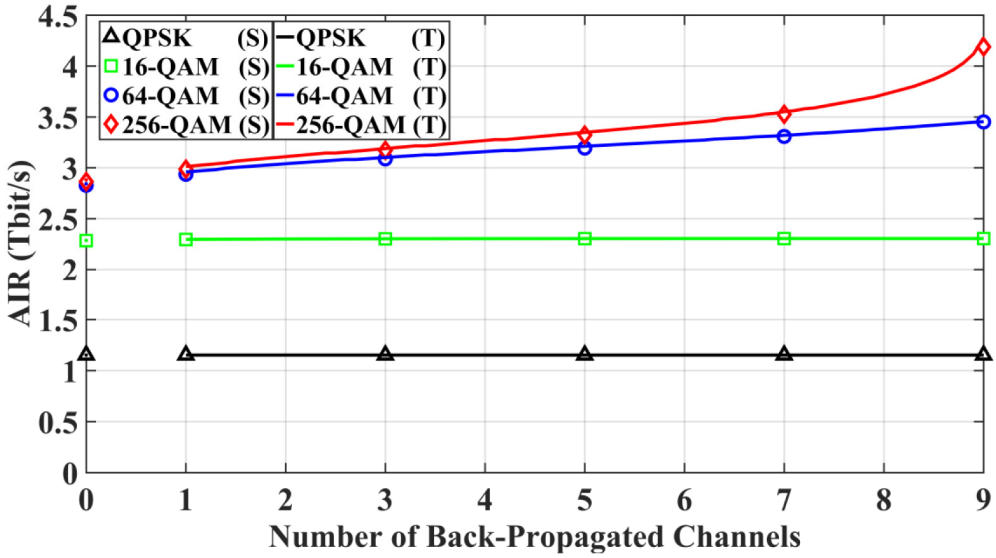

Fig. 7. Analytical and simulation results of AIRs (at optimum optical launch power) versus back-propagated number of channels for different modulation formats. Transmission distance is 2000 km. S: simulation results, T: theoretical model.

The analytical model is further applied to predict the AIRs of the 9-channel 32-Gbaud Nyquist-spaced optical communication systems with different transmission distances, where the use of EDC, partial-bandwidth DBP and full-field DBP has been taken into consideration. The system is estimated under transmission over SSMF with a uniform span length of 80 km. The prediction of AIRs versus transmission distances is illustrated in Fig. 8. It can be seen that, at the transmission distance of 2000 km the DP-256QAM system using 7-channel DBP outperforms the DP-64QAM using full-field (9-channel) DBP, and at the transmission distance of 1200 km the DP-256QAM system using 3-channel, 5-channel and 7-channel DBP all outperforms the DP-64QAM system using full-field (9-channel) DBP. This offers a trade-off on the selection of modulation formats and back-propagated bandwidths to achieve a target AIR. For longer transmission distances, e.g., over 2500 km, only the full-field DBP of DP-256QAM system can outperform the AIR of DP-64QAM system using full-field DBP. In addition, it can be found that for the DP-QPSK modulation format, the system using EDC, partial-bandwidth DBP and full-field DBP shows the same AIR, with the transmission distance up to 6000 km. This means that in an ideal system (no transceiver SNR limitations)

Optics EXPRESS

the application of DBP is not necessary for DP-QPSK transmission to compensate fibre nonlinearities for enhancing the AIR, when the distance is less than 6000 km.

Although the above discussions are analysed based on ideal transmission systems, where the transceiver SNR penalty, DGD, and laser phase noise have been neglected, this paper gives an insight into the optimisation of MC-DBP, as well as in the selection of modulation formats and back-propagated bandwidths when designing practical optical communication systems using digital nonlinearity compensation techniques.

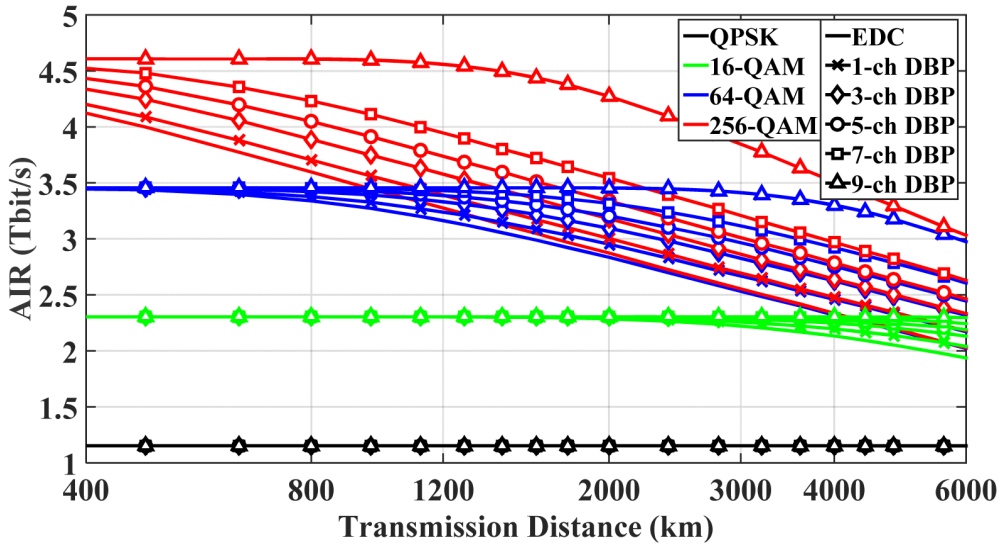

Fig. 8. Analytical prediction of AIRs versus transmission distances at different back-propagated bandwidths for different modulation formats.

The ideal implementations of both optical transmission systems and MC-DBP have been applied in order to investigate the dependence on modulation formats, when an optimum system performance is obtained. The use of 800 step/span in MC-DBP is to ensure the optimal performance of nonlinearity compensation. However, in commercial communication systems, a more feasible and promising value for the number of step per span in the application of MC-DBP is generally considered as 1 step/span [13]. From Fig. 4, it can be found that in such case only 1-channel DBP can give improvement in the system performance compared to the EDC case, which is consistent with our previous work [16]. The performance of optical communication system using the 1 step/span 1-channel DBP is further investigated in terms of SNRs (in Fig. 9) and AIRs (in Fig. 10). Modulation formats of DP-QPSK, DP-16QAM, DP-64QAM, and DP-256QAM are applied, and the transmission distance is again 2000 km. It can be found in Fig. 9 that, similar to the ideal MC-DBP, the DP-16QAM, DP-64QAM, and DP-256QAM systems still behave almost the same, while the DP-QPSK system outperforms the other modulation formats. In Fig. 10, the use of the 1 step/span 1-channel DBP can only produce a small improvement (~0.05 Tbit/s) on the optimum AIRs in the DP-64QAM and DP-256QAM systems, which is from 2.83 Tbit/s at −2 dBm (EDC) to 2.88 Tbit/s at −1.5 dBm (1-channel DBP) in DP-64QAM system, and is from 2.86 Tbit/s at −2 dBm (EDC) to 2.91 Tbit/s at −1.5 dBm (1-channel DBP) in DP-256QAM system.

Some research was also carried out to further reduce the complexity of DBP to 1 step per whole link, which is called single-step DBP. The performance of single-step DBP has been investigated in the DP-QPSK optical transmission system using an enhanced split-step Fourier method [45,46]. The performance dependence of modulation format for this single-step DBP approach will be investigated in our future work.

Optics EXPRESS

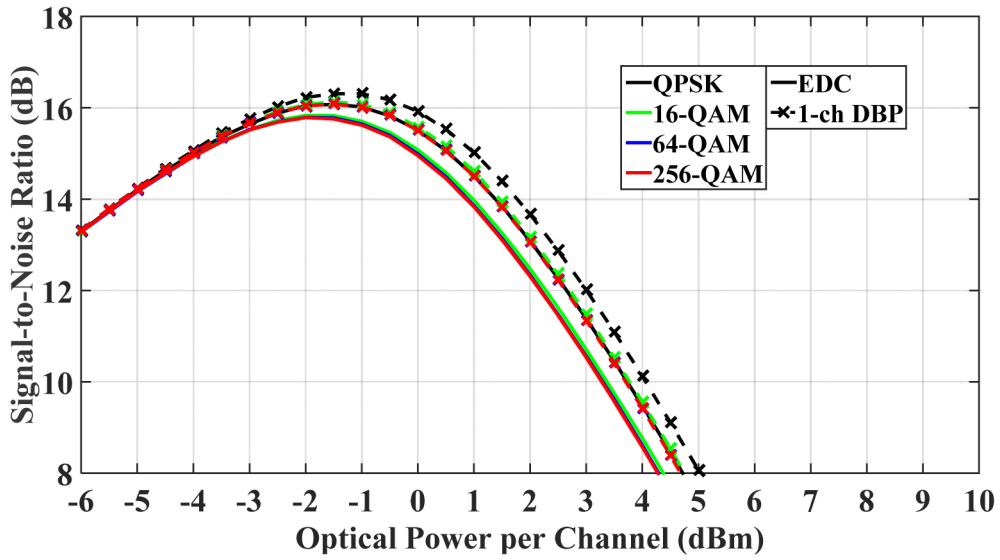

Fig. 9. Simulation results of SNR versus optical launch power using 1-channel DBP for different modulation formats. (The transmission distance is 2000 km, and the 1-channel DBP is applied with 1 step/span).

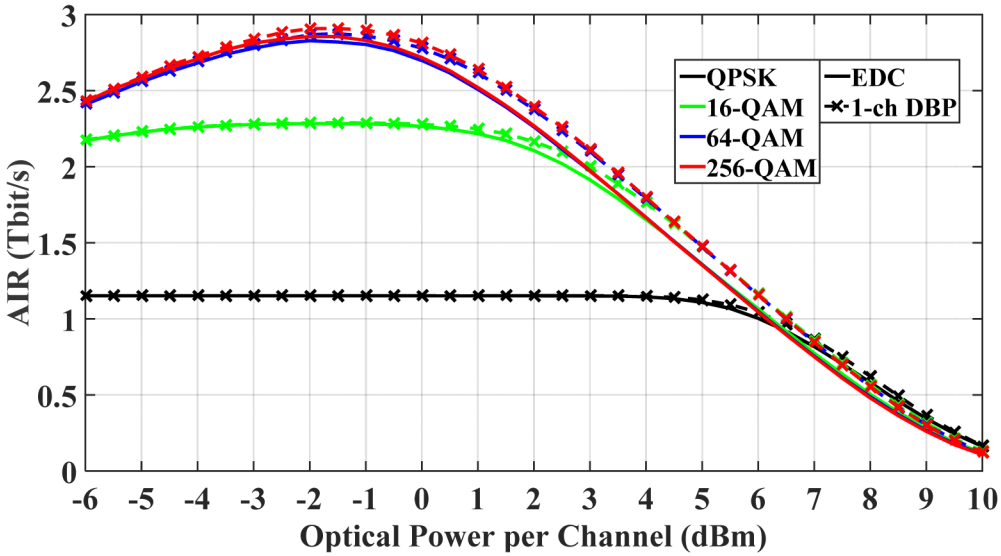

Fig. 10. Simulation results of AIR versus optical launch power using 1-channel DBP for different modulation formats. (The transmission distance is 2000 km, and the 1-channel DBP is applied with 1 step/span).

5. Conclusions

In this paper, the performance and the optimisation of MC-DBP was investigated with respect to both SNR and AIR of the optical fibre communication systems using different modulation formats, such as DP-QPSK, DP-16QAM, DP-64QAM, and DP-256QAM. Numerical simulations and analytical modelling have been carried out in a 9-channel 32-Gbaud Nyquist-spaced SSMF optical communication system. Simulation results show that the nonlinear distortions in the system using full-field DBP (from signal-noise interactions) behave independent of modulation formats, while the nonlinear distortions in the cases of EDC and

Optics EXPRESS

partial-bandwidth DBP (mainly from signal-signal interactions) still show considerable dependence on modulation format. The minimum required number of steps per span in the MC-DBP algorithm has been studied with respect to the AIR of the compensated communication systems. It has been found that the MRNSPS at different back-propagated bandwidths shows a strong dependence on the modulation format, in contrast to the analysis that the MRNSPS at different back-propagated bandwidths is independent of modulation format when the MC-DBP is optimised in terms of SNR. In addition, the analytical model for predicting the performance of EDC and MC-DBP in the optical transmission system has been carried out based on the analysis of modulation format dependent nonlinear distortions. Good agreement has been achieved between the analytical predictions and numerical simulations. According to the analytical prediction, to achieve a given AIR, there would exist a possible trade-off between the modulation format and back-propagated bandwidth, according to practical limitations. Also in an ideal system, DBP is not necessary to compensate the fibre nonlinearities for enhancing the AIR in DP-QPSK transmission, when the distance is less than 6000 km.

Although the analysis and discussions were carried out based on the scheme of ideal transmitter and DSP to study the performance dependence on modulation formats, this paper gives an insight into the optimisation of MC-DBP, as well as in the selection of modulation formats and back-propagated bandwidths for designing practical optical communication systems using digital nonlinearity compensation techniques.

In addition, to analyse a more practical case, the application of 1 step/span in the DBP has also been studied in the Nyquist-spaced optical communication system. It is found that only 1-channel DBP can give improvement in the system performance compared to the EDC case. At the transmission distance of 2000 km, only a small improvement (~0.05 Tbit/s) on the optimum AIRs can be obtained in the DP-64QAM and DP-256QAM systems.

Funding

UK Engineering and Physical Sciences Research Council (EPSRC) Programme Grant UNLOC (EP/J017582/1).